Evolution of Apparent Diffusion Coefficient, Diffusion-weighted, and T2-weighted Signal Intensity of Acute Stroke

Maarten G. Lansberg, Vincent N. Thijs, Michael W. O'Brien, Juan O. Ali, Alex J. de Crespigny, David C. Tong, Michael E. Moseley, and Gregory W. Albers

BACKGROUND AND PURPOSE: Serial study of such MR parameters as diffusion-weighted imaging (DWI), apparent diffusion coefficient (ADC), ADC with fluid-attenuated inversion recovery (ADC_{FLAIR}), and T2-weighted imaging may provide information on the pathophysiological mechanisms of acute ischemic stroke. Our goals were to establish the natural evolution of MR signal intensity characteristics of acute ischemic lesions and to assess the potential of using specific MR parameters to estimate lesion age.

METHODS: Five serial echo-planar DWI studies with and without an inversion recovery pulse were performed in 27 patients with acute stroke. The following lesion characteristics were studied: 1) conventional ADC (ADC_{CONV}); 2) ADC_{FLAIR}; 3) DWI signal intensity (SI_{DWI}); 4) T2-weighted signal intensity (SI_{T2}), and 5) FLAIR signal intensity (SI_{FLAIR}).

RESULTS: The lesion ADC_{CONV} gradually increased from low values during the first week to pseudonormal during the second week to supranormal thereafter. The lesion ADC_{FLAIR} showed the same pattern of evolution but with lower absolute values. A low ADC value indicated, with good sensitivity (88%) and specificity (90%), that a lesion was less than 10 days old. All signal intensities remained high throughout follow-up. SI_{DWI} showed no significant change during the first week but decreased thereafter. SI_{T2} initially increased, decreased slightly during week 2, and again increased after 14 days. SI_{FLAIR} showed the same initial increase as the SI_{T2} but remained relatively stable thereafter.

CONCLUSION: Our findings further clarify the time course of stroke evolution on MR parameters and indicate that the ADC map may be useful for estimating lesion age. Application of an inversion recovery pulse results in lower, potentially more accurate, absolute ADC values.

A detailed understanding of the natural evolution of MR signal intensity parameters in stroke patients is potentially clinically relevant. First, it may provide important information about the time course of ischemic brain damage (1–4), since changes in

MR parameters reflect histopathologic changes in the brain tissue. Several studies have suggested that regions at risk for cerebral infarction may be differentiated from irreversibly damaged tissue when data from different MR techniques are assessed in conjunction (4–8). Information regarding the age of potentially salvageable tissue may be useful to establish rational time windows for stroke treatment and to identify patients who are most likely to benefit from acute stroke therapies. Second, knowledge of the natural evolution of MR characteristics may help estimate the age of a lesion when the time of symptom onset is unclear or when multiple lesions are present that could have different times of onset. Finally, to correctly interpret the results of studies that use MR imaging to monitor the effects of stroke therapies (9–15) it is important to establish the natural evolution of MR parameters in patients not treated with thrombolytic agents or investigational neuroprotective drugs.

Diffusion-weighted imaging signal intensity (SI_{DWI}) and the apparent diffusion coefficient

(ADC) are of particular interest, because these parameters show changes in ischemic brain tissue within hours after symptom onset, when no abnormalities are typically seen on conventional MR images (16–23). Acute ischemic lesions are characterized by a high signal on DWI and a low ADC (16). The ADC, a measure of the freedom of water diffusion, is believed to be low because of a shift of water, within hypoxic brain parenchyma, from the extracellular to the intracellular compartment, where water diffusion is relatively restricted (16).

The natural evolution of the ADC has been studied in animal models (1–3, 16, 24–26) and in stroke patients (4, 17–19, 21, 27–29). However, most human studies have been retrospective and, generally, few scans were obtained per patient, although Schwamm et al (29) conducted a prospective study with repeated imaging during the first week after stroke onset in 14 patients. Results have differed among investigators. Although it is well accepted that ADC values decline rapidly after the onset of ischemia and subsequently increase, the observed time course of the ADC increase to supranormal values has varied from 24 hours (4) to 17 days (29). In addition, the effect that CSF partial volume contamination may have on ADC measurements (30) has not been investigated. The evolution of SI_{DWI} has been studied in a rat model of cerebral ischemia (26), but, to our knowledge, has not previously been analyzed in humans. The evolution of T2-weighted signal intensity (SI_{T2}) of lesions has been described in a few animal models (1, 24, 26) and in one small human study (21).

The primary aim of this prospective cohort study was to determine the evolution of the following characteristics of acute ischemic lesions in stroke patients who were not treated with thrombolytic agents or investigational neuroprotective agents: 1) ADC determined from a conventional ADC map (ADC_{CONV}); 2) ADC determined from a fluid-attenuated inversion recovery (FLAIR) ADC map (ADC_{FLAIR}); 3) signal intensity on DWI MR images (SI_{DWI}); 3) signal intensity on T2-weighted MR images (SI_{T2}), and 4) signal intensity on T2-weighted FLAIR MR images (SI_{FLAIR}). We used these data to investigate whether MR parameters can accurately estimate the age of an ischemic lesion.

Methods

Consecutive patients who presented to the Stanford Stroke Center with a presumed diagnosis of acute stroke within 48 hours after symptom onset were eligible to be considered for this study. Time of stroke onset was determined to be the time at which the patient was last known to be symptom free. A requirement for inclusion in the study was that the actual time of symptom onset had to be known to be accurate within 8 hours. To be eligible for this study, a patient had to have a lesion consistent with an acute stroke in a region appropriate to the presenting symptoms on the baseline DWI study. Patients were excluded if the MR image revealed a nonischemic lesion that could have been responsible for the qualifying symptoms. Patients who were pregnant or less than 18 years

old were excluded, as were patients with active seizures, hypoglycemia (serum glucose < 50 mg/dL), severe coexisting systemic disease, or contraindications to MR imaging (claustrophobia, pacemaker, etc). Patients receiving recombinant tissue plasminogen activator (rtPA) or an investigational neuroprotective agent were also ineligible. Use of anticoagulants or antiplatelet agents was allowed. Guidelines established by the Trial of Org 10172 in Acute Stroke Treatment (TOAST) were used to classify stroke origin (31). Consent for participation in this investigation was obtained from the patient or a legally authorized representative in all cases. The DWI MR protocol was approved by the Stanford University Medical Center human subjects committee.

Five successive MR studies were scheduled for each patient: an initial study within 48 hours of symptom onset and subsequent studies 12 to 48 hours, 3 to 4 days, 5 to 7 days, and 30 days afterward. Examinations could be delayed or canceled on the basis of a patient's request or scheduling conflicts.

MR imaging studies were performed on a 1.5-T unit with gradient strengths of 22 mT/m. A single-shot spin-echo echo-planar DWI sequence (EPI-DWI) was used. The DWI examination acquired 16 slices (5-mm thick with a 2.5-mm gap between slices) with parameters of 6000/110 (TR/TE), a field of view of 24 cm, a bandwidth of 100 kHz, and a matrix of 128 × 128. For each slice, two diffusion weightings (b = 0 and b = 849 mm²/s) were applied along the *x, y,* and *z* axes. This was repeated with the application of an inversion recovery (IR) pulse before excitation for a second set of images. The DWI images with a high b value were unwarped with reference to the b = 0 image to correct for distortions due to eddy currents from the diffusion gradients (32) before ADC calculations. For both sets of images (with and without the IR pulse), three ADC maps were calculated and subsequently averaged to yield two sets of trace images: the conventional trace ADC map and the FLAIR trace ADC map. Furthermore, the three DWI images were averaged to yield an average, isotropic, DWI image. The b = 0 images, acquired with and without the IR pulse, were used as FLAIR and T2-weighted images, respectively.

Data analysis was performed using MR Vision software (MR Vision, Menlo Park, CA) on a Sun Sparc workstation (Sun, Palo Alto, CA). The average ADCs (mm²/s) and signal intensities (arbitrary units) of the ischemic lesions were determined at all time points. Control values were obtained from corresponding normal regions in the contralateral hemisphere. Each measurement was performed by at least two independent, trained observers and their results were averaged. Relative ADCs ($rADC_{CONV}$ and $rADC_{FLAIR}$) and relative SIs (rSI_{T2}, rSI_{FLAIR}, and rSI_{DWI}), quotients of the lesion, and control values were calculated before graphing and statistical analyses.

The ADC and signal intensity values of ischemic lesions represent an area-weighted average determined across all slices. To obtain the weighted average, a region of interest (ROI) was hand drawn within the visually identified ischemic lesion on each slice of the DWI, T2-weighted, and FLAIR sequences. Each ROI was drawn approximately two pixels inward from the lesion edge, excluding CSF and areas of petechial hemorrhage, if present. For each ROI, the average signal intensity (arbitrary units) and the surface area (mm²) were determined. When multiple acute lesions were seen in the same hemisphere, these were outlined individually, yielding several ROIs per slice. Using these data, average area-weighted T2-weighted, FLAIR, and DWI signal intensities for the entire ischemic lesion were calculated. To determine the average ADC_{CONV} and ADC_{FLAIR}, the ROI drawn on the DWI image was transferred to the ADC maps. For MR studies performed beyond day 20, the ROI drawn on the FLAIR image was used to determine the ADC values. Again, average ADC values were obtained by calculating area-weighted averages of the ADC values of all ROIs. This same method was used to generate intensity values and ADCs of the contralateral control regions.

Data were stratified into six time periods: day 1, day 2, days 3 to 4, days 5 to 7, days 8 to 14, and day 14 or more after symptom onset. SigmaStat software (San Rafael, CA) was used for statistical analysis. The mean, standard deviation, and 95% confidence intervals of the mean were calculated for the rADCs and rSIs of each time period. The mean ADCs and SIs of ischemic lesions were compared with control values using a two-tailed paired t-test. The mean $rADC_{CONV}$, $rADC_{FLAIR}$, rSI_{T2}, rSI_{FLAIR}, and rSI_{DWI} were compared among time groups using one-way analysis of variance (ANOVA). If the ANOVA was significant, pairwise comparisons were performed to identify specific time groups with different ADCs or SIs. All tests were performed with $\alpha = .05$.

We performed a linear regression analysis of the time of imaging versus ADC stratified by stroke etiologic subtype to evaluate whether the ADC evolution of these subtypes differed. We compared the slopes of the regression equations for each etiologic subtype (TOAST criteria) with the test for homogeneity of regression coefficients. If the slopes were similar, a differential evolution was unlikely. The same technique was used to study the evolution of ADCs over time with regard to the location of the lesion (subcortical versus cortical) and the baseline National Institutes of Health Stroke Scale (NIHSS) score (comparison of tertiles of NIHSS scores).

The time period that was most accurately characterized by a lesion rADC less than 1.0 (hypointense lesion on the ADC map) was determined with ROC analysis, as were the optimal rSI_{DWI} criteria to characterize this time period. In addition, the time period that could be characterized most accurately by rSI_{T2} or rSI_{FLAIR} criteria was determined. Sensitivity and specificity were calculated for these algorithms.

Results

Thirty patients were enrolled in the study and 27 were included in this analysis. One patient was excluded because the family withdrew consent after the first imaging examination. The second excluded patient was found to have experienced waxing and waning symptoms for approximately 7 days, making the actual time of symptom onset uncertain. The third patient had an extensive hemorrhagic conversion of the infarct that interfered with a determination of signal intensity and ADC values. A total of 123 MR images were obtained, and all but one showed at least one ischemic lesion. The single image with negative findings was obtained 24 days after symptom onset in a patient with a small subcortical infarct on previous images. Twenty-three (85%) of the 27 patients had at least four serial MR studies. The remaining three patients completed three of the five planned MR examinations. Two of these three patients died after their third MR examination, and the other patient missed two examinations because of scheduling conflicts. One patient had two acute symptomatic ischemic lesions, one in each hemisphere, which were analyzed separately. Although lesions were present in both hemispheres, appropriate control regions of unaffected brain parenchyma could still be obtained.

The mean patient age was 72 ± 12 years and the median NIHSS score was 7 (range, 1–24). According to the TOAST classification, the stroke subtype was large artery atherosclerosis in six patients (23%) and cardioembolic in seven patients (26%). One patient (3%) had a stroke of another determined etiology (primary CNS vasculitis). The stroke was considered cryptogenic in 11 patients (41%). Two patients had small vessel disease (7%). The median lesion volume on the baseline DWI was 9.6 cm^3 (range, 1–135). The mean time from symptom onset to the first MR examination was 30 ± 17 hours. Two patients completed the first MR study after 48 hours, one patient at 57 hours, and one patient at 92 hours. The mean time from symptom onset to the second, third, fourth, and final MR studies was 2.9 ± 1.3, 6.4 ± 4.7, 8.5 ± 4.6, and 34.0 ± 9.7 days, respectively.

ADC_{CONV} and ADC_{FLAIR}

During the first 7 days after symptom onset, the mean ADC_{CONV} and ADC_{FLAIR} of ischemic brain lesions were significantly lower than those of contralateral control regions ($P < .001$). From days 8 to 14, the mean ADC_{CONV} and ADC_{FLAIR} did not differ significantly from that in the control regions ($P = .874$); beyond 14 days, both the mean ADC_{CONV} and ADC_{FLAIR} were significantly higher than that in control regions ($P < .001$). At these chronic time points, discrimination of lesions from adjacent CSF was, in some instances, easier on the FLAIR ADC map than on the conventional ADC map (Fig 1). Figure 2A shows the evolution of $rADC_{CONV}$ and $rADC_{FLAIR}$. A progressive increase in rADC values was observed. The mean rADCs for all time groups beyond 4 days were statistically significantly higher than the mean rADC during day 1.

The mean ADC_{CONV} control value, calculated using all 123 MR studies, was higher than the ADC_{FLAIR} control value ($876 \pm 84 \times 10^{-6}$ mm^2/s versus $821 \pm 85 \times 10^{-6}$ mm^2/s, $P < .001$). Table 1 shows a comparison of the ADC_{CONV} and the ADC_{FLAIR} for cortical and subcortical lesions and for large lesion volumes and small lesion volumes. On average, the ADC_{FLAIR} was lower than the ADC_{CONV} within the ischemic lesions. This effect was most marked in cortical lesions as compared with subcortical lesions. The difference between ADC_{FLAIR} and ADC_{CONV} was also greatest in the lesions with the largest volumes. As large lesions have a higher probability of being in contact with CSF spaces, these findings suggest that the ADC_{FLAIR} avoids contamination of CSF within the ADC maps.

The shift from rADC values less than 1.0 to values over 1.0 occurred between days 5 and 14 after symptom onset. The earliest time that an $rADC_{CONV}$ greater than 1.0 was observed was at 109 hours. Subsequently, the frequency of lesions with an $rADC_{CONV}$ over 1.0 gradually increased from 25% (7/28) for lesions imaged between days 5 through 7, to 55% (6/11) between days 8 through 14, to 93% (25/27) after day 14. For the $rADC_{FLAIR}$ these values were 25%, 73%, and 93%, respectively. Of the two patients with low ADCs
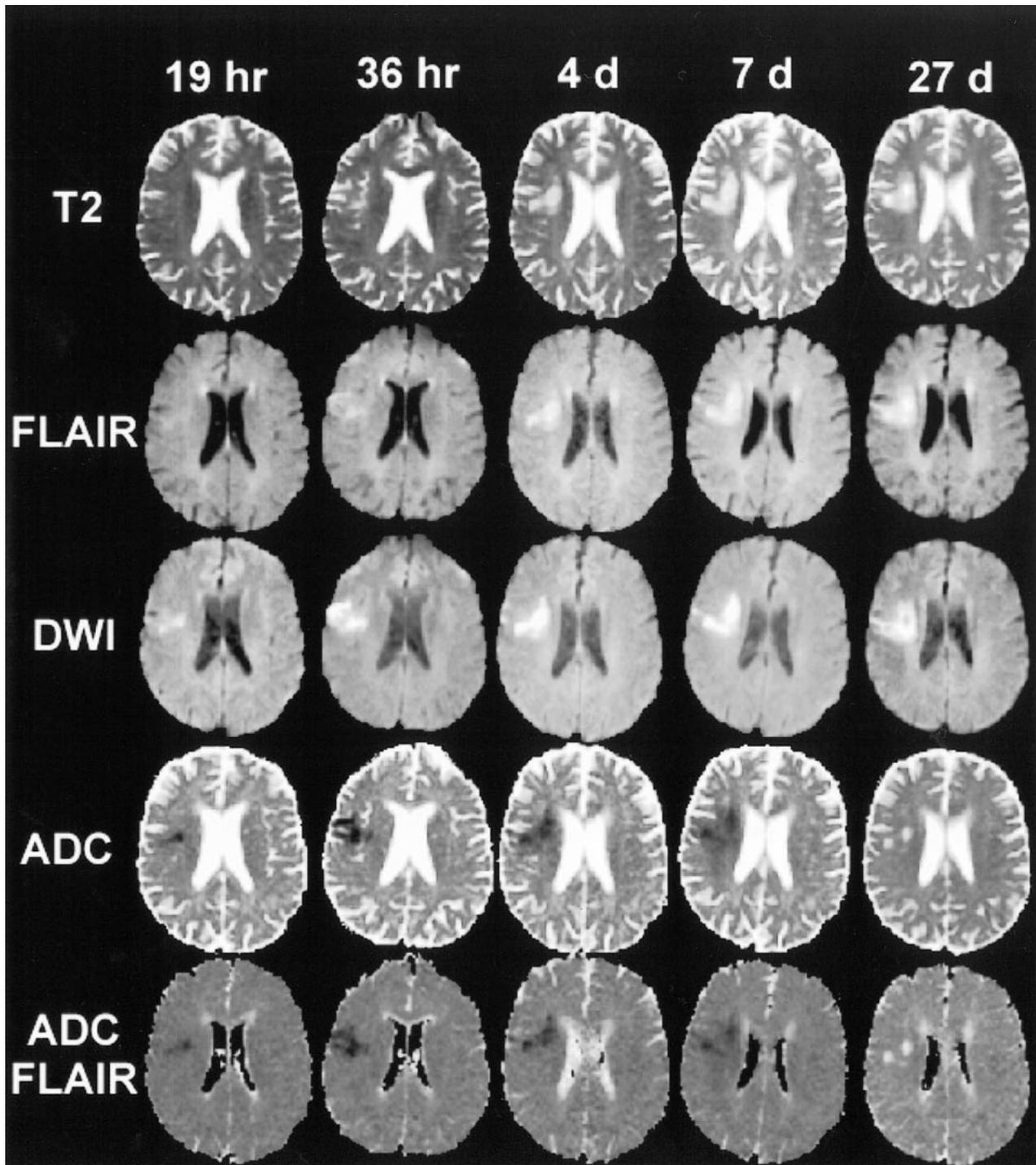
FIG 1.   MR images (6000/210/1) at five subsequent time points in a 67-year-old woman with left hand weakness, left facial droop, and slurred speech. This example shows the typical evolution of the SI_{T2} (*top row*), SI_{FLAIR} (*second row*), SI_{DWI} (*third row*), ADC_{CONV} (*fourth row*), and ADC_{FLAIR} (*bottom row*) of an acute ischemic lesion (right hemisphere). On the ADC maps, the lesion is hypointense up to day 7 and hyperintense at 27 days, making it possible to differentiate the acute from the chronic lesion. On the DWI images, the lesion is hyperintense at all time points so that, by visual inspection, the signal intensity of the lesion on the acute scan cannot be differentiated from that on the chronic scan. On the T2-weighted and FLAIR images, lesion signal intensity increases up to day 4 and remains high thereafter. Note that at 27 days the lesion is more identifiable on the ADC_{FLAIR} map than on the ADC_{CONV} map.

after 14 days, one was imaged at 20 days and had an $rADC_{CONV}$ of 0.89 ($rADC_{FLAIR}$ 0.95) and the other was imaged at 33 days and had an $rADC_{CONV}$ of 0.84 ($rADC_{FLAIR}$ 0.83). Lesions with an r-ADC_{CONV} or $rADC_{FLAIR}$ of less than 1.0 most ac-

curately (least false positive or false negative) characterized the time period from 0 to 10 days after symptom onset. Considering lesions with an r-ADC_{CONV} of less than 1.0 to be 10 days old or less and considering lesions with an $rADC_{CONV}$ of 1.0
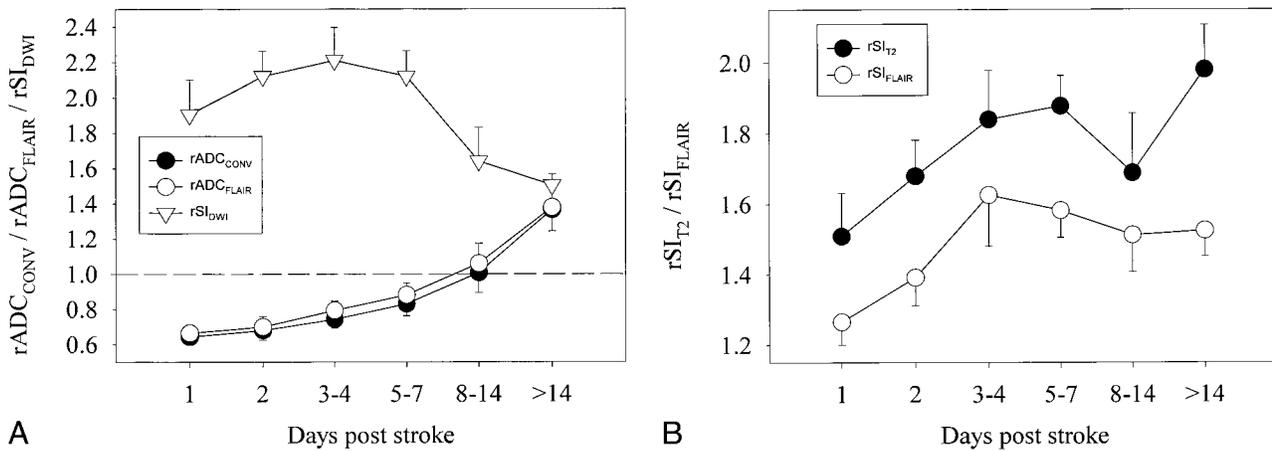
FIG 2. Average relative lesion ADC values and signal intensities with 95% confidence intervals during five time intervals after onset of stroke symptoms.

A, $rADC_{CONV}$, $rADC_{FLAIR}$, and rSI_{DWI}.

B, rSI_{T2} and rSI_{FLAIR} (see Table 2 for the number of lesions included at each time interval).

to be more than 10 days old yielded 88% sensitivity and 90% specificity. Using an $rADC_{FLAIR}$ cutoff of 1.0 yielded very similar results (sensitivity 86%, specificity 93%).

ADC Evolution in Stroke Subtypes

Regression analysis determined that the evolution of ADC over time was similar for patients with cardioembolic stroke, for patients with large vessel disease, and for patients with cryptogenic stroke, small vessel disease, or other determined pathogeneses of stroke (test for homogeneity of regression coefficients, $P = .388$).

No differential evolution could be found for subcortical versus cortical lesions or for increasing severity of the baseline NIHSS score (test for homogeneity of regression coefficients, $P = .482$ for location and $P = .697$ for NIHSS score).

SI_{DWI}

The mean SI_{DWI} was significantly higher than control values throughout all time periods. The lowest rSI_{DWI} was 1.18 and was seen in a lesion imaged 30 days after symptom onset. Figure 2A illustrates the evolution of the rSI_{DWI}. The mean rSI_{DWI} of lesions, examined during day 1, day 2, days 3 to 4, and days 5 through 7, ranged from

1.90 to 2.21 (Table 2), and no significant differences were found among groups. In the 8- to 14-day period, the mean rSI_{DWI} decreased to 1.64 ± 0.28, and was significantly lower than during the earlier time periods ($P < .001$). After day 14, mean rSI_{DWI} further decreased to 1.50 ± 0.16, but this was not significantly lower than during the 8- to 14-day period ($P = .07$). On the latest study in this series, 72 days after symptom onset, the rSI_{DWI} was 1.42.

Lesions less than 10 days old could be differentiated from those more than 10 days old by using rSI_{DWI}. Maximal accuracy was achieved when lesions with an rSI_{DWI} of more than 1.68 were considered to be 10 days old or less, while lesions with an rSI_{DWI} of less than 1.68 were considered to be 10 days old or older. This algorithm was 85% sensitive and 90% specific.

SI_{T2} and SI_{FLAIR}

SI_{T2} and SI_{FLAIR} were significantly higher than control values for all time periods. However, on the baseline MR study, the hyperintensity was often so subtle that the lesion could not be identified by visual inspection (Fig 1). In these instances, the ROI from the DWI image was transferred to the T2-weighted and FLAIR images for signal intensity measurement. Figure 2B shows that the rSI_{T2} grad-

TABLE 1: Comparison of ADC_{FLAIR} with ADC_{CONV} with respect to lesion location (cortical and subcortical) and lesion size (highest tertile of baseline DWI volume and lowest and middle tertile of baseline DWI volume)

	$ADC_{FLAIR(\mu mm^2/s)}$	$ADC_{CONV(\mu mm^2/s)}$	*P* Value
Cortical and subcortical lesions (mean, SD)	765 ± 264	785 ± 282	.003
Cortical lesions (mean, SD)	793 ± 279	817 ± 295	.006
Subcortical lesions (mean, SD)	689 ± 204	700 ± 227	.210
Largest baseline DWI lesion volumes, highest tertile (mean, SD)	504 ± 29	537 ± 33	.006
Smallest baseline DWI lesion volumes, lowest and middle tertile (mean, SD)	590 ± 120	601 ± 99	.529

Note.—The highest tertile of lesion volumes is the baseline DWI volume of 16 to 135 cm³; the lowest and middle tertile of lesion volumes are the baseline lesion DWI volumes of 1 to 11.5 cm³.

TABLE 2: Summary of average relative apparent diffusion coefficient and signal intensity values (±SD) of ischemic lesions during different time intervals

Days after Stroke	No. of Lesions	rADC (mean ± SD)	rADC_FLAIR (mean ± SD)	rSI_DWI (mean ± SD)	rSI_T2 (mean ± SD)	rSI_FLAIR (mean ± SD)
1	14	0.64 ± 0.08	0.66 ± 0.08	1.90 ± 0.34	1.51 ± 0.21	1.27 ± 0.07
2	20	0.68 ± 0.12	0.70 ± 0.13	2.12 ± 0.30	1.68 ± 0.22	1.39 ± 0.17
3–4	22	0.74 ± 0.12	0.79 ± 0.12	2.21 ± 0.42	1.84 ± 0.31	1.63 ± 0.33
5–7	28	0.83 ± 0.18	0.88 ± 0.17	2.12 ± 0.37	1.88 ± 0.22	1.58 ± 0.20
8–14	11	1.01 ± 0.17	1.06 ± 0.17	1.64 ± 0.28	1.67 ± 0.25	1.51 ± 0.16
>14	27	1.37 ± 0.31	1.38 ± 0.32	1.50 ± 0.16	1.98 ± 0.32	1.51 ± 0.23

Note.—$rADC_{CONV}$ indicates relative conventional apparent diffusion coefficient; $rADC_{FLAIR}$, relative fluid-attenuated inversion recovery apparent diffusion coefficient; rSI_{DWI}, relative diffusion-weighted signal intensity; rSI_{T2}, relative T2-weighted signal intensity; rSI_{FLAIR}, relative fluid-attenuated inversion recovery signal intensity.

ually increased over the first week from 1.51 ± 0.21 to 1.88 ± 0.22, while the rSI_{FLAIR} increased from 1.27 ± 0.07 to 1.58 ± 0.20. The rSIs of the 3- to 4-day period and the 5- to 7-day period were significantly higher than those during day 1. Compared with the 5- to 7-day period, slightly lower signal intensities were seen during the 8-to 14-day period (rSI_{T2} = 1.67 and rSI_{FLAIR} = 1.51), but these differences were not statistically significant. After day 14, the rSI_{T2} increased significantly to 1.98 ± 0.32, whereas the rSI_{FLAIR} remained stable at 1.51 ± 0.23. In the control regions, the mean SI_{T2} was higher than the mean SI_{FLAIR} (309 ± 135 versus 238 ± 102, $P < .001$).

The early rise in SI_{T2} made it possible to differentiate acute lesions from older lesions based on rSI_{T2} or rSI_{FLAIR}. Maximal accuracy was achieved when lesions with an rSI_{T2} of less than 1.52 were considered to be 36 hours old or less, while lesions with an rSI_{T2} of 1.52 or greater were considered to be more than 36 hours old. This algorithm was 67% sensitive and 90% specific. Considering lesions with an rSI_{FLAIR} of less than 1.37 to be 36 hours old or less, while considering lesions with an rSI_{FLAIR} of 1.37 or greater to be less than 36 hours old yielded 91% sensitivity and 83% specificity.

Discussion

Our results show that in stroke patients who are not treated with thrombolytic agents or investigational neuroprotective agents the mean rADC of ischemic lesions gradually increases over time, but remains significantly decreased relative to that of a contralateral control region for the first 7 days after symptom onset. This pattern is consistent with several previous studies (17–19, 21, 27). An earlier rise in ADC has been reported by two groups (4, 28) but most likely reflects differences in methods of data acquisition (33) and data analysis (34). The later rise in ADC observed in one recent study with a relatively small sample size may have been a coincidental finding (29).

Our study also shows that the SI_{T2} of ischemic lesions increases progressively over the first 4 days after symptom onset and remains relatively stable thereafter. The increase in mean SI_{T2} over the first

4 days, with a relatively stable ADC, may be explained by a simultaneous increase in cytotoxic and vasogenic edema. Clinically, this corresponds well with the typical evolution of brain swelling that is often observed in large infarcts over the initial 2- to 5-day period after symptom onset (35, 36). Peaking of SI_{T2} and return of the ADC to (pseudo) normal values have been shown to correlate histologically with the appearance of large numbers of shrunken eosinophilic neurons, indicating irreversible neuronal damage in a rat stroke model (1). In rats, these changes in MR parameters occur approximately 24 hours after stroke onset, whereas our data indicate that these MR findings in humans typically do not occur until 4 days after symptom onset. This suggests a considerably longer evolution of the ischemic lesion and potentially a longer time window during which effective therapies might be beneficial in humans. Note, however, that different regions within an ischemic lesion may progress at a different pace, possibly because of varying degrees of hypoperfusion or intrinsic differences in tissue vulnerability to hypoxia. An MR tissue signature model has been proposed to account for these regional differences and may be a more sensitive indicator of potentially salvageable tissue (4, 8).

In this series, signal intensity on DWI images showed little change during the first week after symptom onset and decreased thereafter, but all lesions remained hyperintense throughout the time of follow-up. This pattern was most likely the result of SI_{DWI} being influenced by two factors: water diffusibility and intrinsic T2 properties (T2 shine-through) of the tissue being examined (37). Because the DWI signal remains hyperintense for a long period (up to 72 days in this study), it is not ideal for estimating lesion age. Using DWI to differentiate lesions less than 10 days old from those more than 10 days old requires the ability to differentiate between very hyperintense ($rSI_{DWI} > 1.68$) and moderately hyperintense ($rSI_{DWI} < 1.68$) signal. In our experience, this is generally not possible by visual inspection alone and thus requires sophisticated ROI analysis, a time-consuming process. In contrast, differentiating lesions equal to or

less than 10 days old from those more than 10 days old based on ADC is relatively simple, because it requires differentiating hypointense from hyperintense. This, in our experience, is usually easily determined on the basis of visual inspection alone. Thus, although one recent study concluded that the DWI image alone (without the ADC map) is sufficient for clinical stroke imaging (38), our results indicate that the ADC map may add useful data regarding the age of ischemic lesions. Based on the SI_{T2}, lesions that are less than 36 hours old can usually be differentiated from those more than 36 hours old. However, this also requires differentiating subtle degrees of hyperintensity, something that is probably not feasible by visual inspection. Further prospective studies will be required to determine the sensitivity and specificity of estimating lesion age on the basis of visual interpretation without ROI analyses.

DWI has been used to monitor stroke treatment in several animal models of reperfusion after cerebral ischemia (13, 14, 39–42). A more rapid increase of the ADC and a less pronounced increase of the SI_{T2} has consistently been found in animals subjected to early reperfusion as compared with permanent occlusion models. Our group recently reported an early rise in ADC in patients treated with rtPA (15). Previous studies have shown that the decrease in ADC during acute ischemia is related to significant reductions in cerebral blood flow (16). ADC and, potentially, other MR parameters are quantitative measures that may be useful for evaluating the effect of stroke treatments. Data from this study may be helpful as historical control values for future treatment studies.

To our knowledge, the application of an IR pulse as part of the EPI-DWI examination has not previously been described in human stroke studies. Application of an IR pulse to suppress the CSF signal resulted in lower ADC values. This strongly suggests that the ADC values obtained from a conventional ADC map are contaminated with CSF signal, an issue first addressed by Pierpaoli et al (30). Thus, the IR pulse may be required to obtain accurate ADC values. Moreover, chronic lesions are frequently better visualized on the FLAIR ADC map than on the conventional ADC map.

This study has some limitations. We have few data regarding the MR characteristics of hyperacute lesions (<12 hours). Patients who presented within 12 hours of symptom onset were often excluded from this natural history study, because they were treated with rtPA or enrolled in investigational stroke treatment trials. Also, because of the predetermined scan time points, we obtained few scans between 15 and 25 days after symptom onset. Further studies are currently underway to analyze these time periods in more detail.

Conclusion

This study documents the natural evolution of ADC_{CONV}, ADC_{FLAIR}, SI_{DWI}, SI_{FLAIR}, and SI_{T2} in acute stroke patients. These data help further clarify the time course of stroke evolution, which may have important implications for establishing rational time windows for acute stroke treatment. In addition, these data could be used as reference values for studies that use MR parameters for the evaluation of stroke therapies. Moreover, these data provide evidence of the importance of the ADC map for approximating lesion age and indicate that FLAIR ADC maps yield lower, potentially more accurate ADC values than do conventional ADC maps.

References

1. Knight RA, Dereski MO, Helpern JA, Ordidge RJ, Chopp M. **Magnetic resonance imaging assessment of evolving focal cerebral ischemia: comparison with histopathology in rats.** *Stroke* 1994;25:1252–1261
2. Pierpaoli C, Righini A, Linfante I, Tao-Cheng JH, Alger JR, Di Chiro G. **Histopathologic correlates of abnormal water diffusion in cerebral ischemia: diffusion-weighted MR imaging and light and electron microscopic study.** *Radiology* 1993;189:439–448
3. Hasegawa Y, Fisher M, Latour LL, Dardzinski BJ, Sotak CH. **MRI diffusion mapping of reversible and irreversible ischemic injury in focal brain ischemia.** *Neurology* 1994;44:1484–1490
4. Welch KM, Windham J, Knight RA, et al. **A model to predict the histopathology of human stroke using diffusion and T2-weighted magnetic resonance imaging.** *Stroke* 1995;26:1983–1989
5. Barber PA, Darby DG, Desmond PM, et al. **Prediction of stroke outcome with echoplanar perfusion- and diffusion-weighted MRI.** *Neurology* 1998;51:418–426
6. Rordorf G, Koroshetz WJ, Copen WA, et al. **Regional ischemia and ischemic injury in patients with acute middle cerebral artery stroke as defined by early diffusion-weighted and perfusion-weighted MRI.** *Stroke* 1998;29:939–943
7. Tong DC, Yenari MA, Albers GW, O'Brien M, Marks MP, Moseley ME. **Correlation of perfusion- and diffusion-weighted MRI with NIHSS score in acute (<6.5 hour) ischemic stroke.** *Neurology* 1998;50:864–870
8. D'Olhaberriague L, Welch KM, Nagesh V, et al. **Preliminary clinical-radiological assessment of a MR tissue signature model in human stroke.** *J Neurol Sci* 1998;156:158–166
9. Yenari MA, Palmer JT, Sun GH, de Crespigny A, Mosely ME, Steinberg GK. **Time-course and treatment response with SNX-111, an N-type calcium channel blocker, in a rodent model of focal cerebral ischemia using diffusion-weighted MRI.** *Brain Res* 1996;739:36–45
10. Lo EH, Pierce AR, Mandeville JB, Rosen BR. **Neuroprotection with NBQX in rat focal cerebral ischemia: effects on ADC probability distribution functions and diffusion-perfusion relationships.** *Stroke* 1997;28:439–446
11. Yenari MA, de Crespigny A, Palmer JT, et al. **Improved perfusion with rt-PA and hirulog in a rabbit model of embolic stroke.** *J Cereb Blood Flow Metab* 1997;17:401–411
12. Takano K, Carano RA, Tatlisumak T, et al. **Efficacy of intra-arterial and intravenous prourokinase in an embolic stroke model evaluated by diffusion-perfusion magnetic resonance imaging.** *Neurology* 1998;50:870–875
13. Busch E, Kruger K, Allegrini PR, et al. **Reperfusion after thrombolytic therapy of embolic stroke in the rat: magnetic resonance and biochemical imaging.** *J Cereb Blood Flow Metab* 1998;18:407–418
14. Jiang Q, Zhang RL, Zhang ZG, Ewing JR, Divine GW, Chopp M. **Diffusion-, T2-, and perfusion-weighted nuclear magnetic resonance imaging of middle cerebral artery embolic stroke and recombinant tissue plasminogen activator intervention in the rat.** *J Cereb Blood Flow Metab* 1998;18:758–767

15. Tong DC, Lansberg MG, Yenari MA, Moseley ME. **Diffusion and perfusion weighted imaging following administration of tissue plasminogen activator (rt-PA) in humans with acute ischemic stroke.** In: *Proceedings of the International Society for Magnetic Resonance in Medicine, 6th Annual Meeting; Sydney, Australia; 1998.* International Society for Magnetic Resonance in Medicine; New York: 1998:238

16. Moseley ME, Cohen Y, Mintorovitch J, et al. **Early detection of regional cerebral ischemia in cats: comparison of diffusion- and T2-weighted MRI and spectroscopy.** *Magn Reson Med* 1990;14:330–346

17. Warach S, Chien D, Li W, Ronthal M, Edelman RR. **Fast magnetic resonance diffusion-weighted imaging of acute human stroke.** *Neurology* 1992;42:1717–1723

18. Warach S, Gaa J, Siewert B, Wielopolski P, Edelman RR. **Acute human stroke studied by whole brain echo planar diffusion-weighted magnetic resonance imaging.** *Ann Neurol* 1995;37: 231–241

19. Marks MP, de Crespigny A, Lentz D, Enzmann DR, Albers GW, Moseley ME. **Acute and chronic stroke: navigated spin-echo diffusion-weighted MR imaging.** *Radiology* 1996;199:403–408

20. Sorensen AG, Buonanno FS, Gonzalez RG, et al. **Hyperacute stroke: evaluation with combined multisection diffusion-weighted and hemodynamically weighted echo-planar MR imaging.** *Radiology* 1996;199:391–401

21. Lutsep HL, Albers GW, DeCrespigny A, Kamat GN, Marks MP, Moseley ME. **Clinical utility of diffusion-weighted magnetic resonance imaging in the assessment of ischemic stroke.** *Ann Neurol* 1997;41:574–580

22. Singer MB, Chong J, Lu D, Schonewille WJ, Tuhrim S, Atlas SW. **Diffusion-weighted MRI in acute subcortical infarction.** *Stroke* 1998;29:133–136

23. Lovblad KO, Laubach HJ, Baird AE, et al. **Clinical experience with diffusion-weighted MR in patients with acute stroke.** *AJNR Am J Neuroradiol* 1998;19:1061–1066

24. Hoehn-Berlage M, Eis M, Back T, Kohno K, Yamashita K. **Changes of relaxation times (T1, T2) and apparent diffusion coefficient after permanent middle cerebral artery occlusion in the rat: temporal evolution, regional extent, and comparison with histology.** *Magn Reson Med* 1995;34:824–834

25. Minematsu K, Li L, Fisher M, Sotak CH, Davis MA, Fiandaca MS. **Diffusion-weighted magnetic resonance imaging: rapid and quantitative detection of focal brain ischemia.** *Neurology* 1992;42:235–240

26. Verheul HB, Berkelbach van der Sprenkel JW, Tulleken CA, Tamminga KS, Nicolay K. **Temporal evolution of focal cerebral ischemia in the rat assessed by T2-weighted and diffusion-weighted magnetic resonance imaging.** *Brain Topogr* 1992;5: 171–176

27. Schlaug G, Siewert B, Benfield A, Edelman RR, Warach S. **Time course of the apparent diffusion coefficient (ADC) abnormality in human stroke.** *Neurology* 1997;49:113–119

28. Chien D, Kwong KK, Gress DR, Buonanno FS, Buxton RB, Rosen BR. **MR diffusion imaging of cerebral infarction in humans.** *AJNR Am J Neuroradiol* 1992;13:1097–1102

29. Schwamm LH, Koroshetz WJ, Sorensen AG, et al. **Time course of lesion development in patients with acute stroke: serial diffusion- and hemodynamic-weighted magnetic resonance imaging.** *Stroke* 1998;29:2268–2276

30. Pierpaoli C, Alger JR, Righini A, et al. **High temporal resolution diffusion MRI of global cerebral ischemia and reperfusion.** *J Cereb Blood Flow Metab* 1996;16:892–905

31. Adams HP Jr, Bendixen BH, Kappelle LJ, et al. **Classification of subtype of acute ischemic stroke: definitions for use in a multicenter clinical trial, TOAST (Trial of Org 10172 in Acute Stroke Treatment).** *Stroke* 1993;24:35–41

32. de Crespigny A, Moseley M. **Eddy current induced image warping in diffusion weighted EPI.** In: *Proceedings of the International Society for Magnetic Resonance in Medicine, 6th Annual Meeting; Sydney, Australia; 1998.* International Society for Magnetic Resonance in Medicine; New York: 1998:661

33. Warach S, Moseley M, Sorensen AG, Koroshetz W. **Time course of diffusion imaging abnormalities in human stroke.** *Stroke* 1996;27:1254–1255

34. Nagesh V, Welch KM, Windham JP, et al. **Time course of ADCw changes in ischemic stroke: beyond the human eye!** *Stroke* 1998;29:1778–1782

35. O'Brien MD. **Ischemic cerebral edema: a review.** *Stroke* 1979; 10:623–628

36. Hacke W, Schwab S, Horn M, Spranger M, De Georgia M, von Kummer R. **"Malignant" middle cerebral artery territory infarction: clinical course and prognostic signs.** *Arch Neurol* 1996;53:309–315

37. Le Bihan D, Breton E, Lallemand D, Grenier P, Cabanis E, Laval-Jeantet M. **MR imaging of intravoxel incoherent motions: application to diffusion and perfusion in neurologic disorders.** *Radiology* 1986;161:401–407

38. Chong J, Lu D, Aragao F, et al. **Diffusion-weighted MR of acute cerebral infarction: comparison of data processing methods.** *AJNR Am J Neuroradiol* 1998;19:1733–1739

39. Mintorovitch J, Moseley ME, Chileuitt L, Shimizu H, Cohen Y, Weinstein PR. **Comparison of diffusion- and T2-weighted MRI for the early detection of cerebral ischemia and reperfusion in rats.** *Magn Reson Med* 1991;18:39–50

40. Minematsu K, Li L, Sotak CH, Davis MA, Fisher M. **Reversible focal ischemic injury demonstrated by diffusion-weighted magnetic resonance imaging in rats.** *Stroke* 1992;23:1304–1310

41. Bizzi A, Righini A, Turner R, et al. **MR of diffusion slowing in global cerebral ischemia.** *AJNR Am J Neuroradiol* 1993;14: 1347–1354

42. Rother J, Waggie K, van Bruggen N, de Crespigny AJ, Moseley ME. **Experimental cerebral venous thrombosis: evaluation using magnetic resonance imaging.** *J Cereb Blood Flow Metab* 1996;16:1353–1361